Remote Sensing of Land
Homepage: www.gathacognition.com/journal/gcj1
http://dx.doi.org/10.21523/gcj1

Original Research Paper

Detection and Delineation of Water Bodies in Hilly Region using CartoDEM, SRTM and ASTER GDEM Data

Sainath Aher[1], Komali Kantamaneni[2], Pragati Deshmukh[3]*

1. Department of Geography, S.N. Arts, D.J.M. Commerce and B.N.S. Science College, Sangamner 422605, India.
2. Maritime, Technology and Environment Hub, Research and Innovation, Southampton Solent University, E Park Terrace, Hampshire SO14 0YN, United Kingdom.
3. Department of Geography, H.P.T. Arts and R.Y.K. Science College, Nashik 422005, India.

Abstract

Detection and delineation of Water Body Area (WBA), particularly over inaccessible hilly region is not always possible in view of time, resources and cost issues. An automated procedure for detection and delineation of water bodies in the hilly region was performed using satellite-derived DEMs. CartoDEM, SRTM and ASTER GDEM data with 30, 90 and 30m resolutions, respectively to generate the Elevation Points Features (EPF) in GIS platform. Total 7194906 EPFs were generated using these three DEMs. Contour and slope maps were also prepared to eliminate the outlier EPFs (non-water bodies) with flattered surface logic. Flattened area on DEMs, connected contour at edges of water bodies and 0° to 0.5° slopping area were considered as WBA in the region (2311 Km^2) of Western Ghat (India). The nearest neighbor to cubic convolution conversion of DEMs was found useful for detection of boundary of water bodies more precisely. These results were validated from Landsat-8 satellite images and topographic maps (Survey of India). About 3.09% from CartoDEM, 2.22% area from ASTER GDEM and 4.38% from SRTM DEM were estimated as WBA. CartoDEM data can be suggested for precise detection of smaller water bodies in hilly region. Methodology formulated in this study could be used as a rapid assessment tool for detection of water bodies, especially in the inaccessible region for better water resources management.

Article history

Received: 06 August 2017
Revised: 26 October 2017
Accepted: 27 October 2017

Keywords

Water bodies;
Digital Elevation Model;
Elevation point feature;
GIS

Editor(s)

V.S. Bhagat

1 INTRODUCTION

Surface water resource is a significant for hydrological cycles, survival of bio-spheres, global warming control and allied socio-economic development. (1) Imbalance between availability and demand for water resources, (2) Degradation of water quality in many of the regions, (3) Depleted and insecure groundwater resources, (4) inter-sector and intra-sector competition and inter-regional and international conflicts are identified common problems in water management sector (Bhagat and Sonawane, 2011; Deshmukh and Aher, 2016). Therefore, precise information about spatial distribution of water bodies is essential for management of several issues related to hydrology and ecology (Ridda and Liu, 1998; Famiglietti and Rodell, 2013) and socio-economic issues like drinking water, agriculture, industry etc. Mapping of surface water bodies at high resolution is essential for the management of drinking water, agriculture, industry, floods, drought, etc. (Du *et al.*, 2012; Sun *et al.*, 2012; Aher *et al.*, 2017) for better water resource management (Feng *et al.*, 2015). Surface and groundwater resources differ according to their distribution and having variations in its physico-climatic elements (Deshmukh and Aher, 2016). The variation in the quality and quantity of surface water is also depends on physiography, land use, land cover and geological structure (Deshmukh et al., 2017). A large number of natural and artificial water bodies (dam) are typically located in the hilly areas. Therefore, detection and delineation of water bodies in these areas are multifactual and time consuming task using conventional

* Author address for correspondence
Department of Geography, H.P.T. Arts and R.Y.K. Science College, Nashik 422005, India.
Tel.: +91 9096244069. Emails: dpragati30@gmail.com (*P. Deshmukh*-Corresponding author); komali.kantamaneni@solent.ac.uk (*K. Kantamaneni*); saigeo23@gmail.com (*S. Aher*)

http://dx.doi.org/10.21523/gcj1.17010103

methods (Cole *et al.*, 2007; Carroll *et al.*, 2011).

In many research projects, trainings and management practices satellite data at different spatial, spectral and temporal resolutions has been used for monitoring, detecting and extracting the water bodies using Geographical Information System (GIS) techniques (Xu, 2006; Tang *et al.*, 2013). Satellite images have been used for: (1) detection and delineation of land use/cover changes (Salmon *et al.*, 2013; Demir *et al.*, 2013; Jawak and Luis, 2013; Deshmukh *et al.*, 2017), forest changes (Kaliraj *et al.*, 2012; Markogianni *et al.*, 2013), potential areas for afforestation (Bhagat, 2009), river bank erosion identification (Aher *et al.*, 2012) (2) monitoring of disasters like floods, droughts (Aher *et al.*, 2017), seismic hazards (Barbara *et al.*, 2016), landslide mapping (Gawali *et al.*, 2017) and forest fires (Volpi *et al.*, 2013; Brisco *et al.*, 2013), and (3) modeling of hydrological, ecological, climatological aspects (Dronova *et al.*, 2011; Zhu *et al.*, 2011) etc. At the same time, several studies (Meijerink, 1996; Ho *et al.*, 2010; Bhagat and Sonwane, 2011; Rokni *et al.*, 2014; Akhtar *et al.*, 2015) show the efficiency of satellite imagery for mapping, monitoring and quantitative appraisal of the water bodies. The detection and delineation of water bodies in the area are consisted with the satellite-derived database and methodology, which could consume the time and resources for micro level assessment of water bodies, especially at inaccessible area.

The majority of the studies conducted for detection and delineation of surface water bodies is based on indices calculated using multiple bands of satellite data (Min *et al.*, 2011). Bhagat and Sonawane (2011) used the Landsat ETM (+) data for delineation of water bodies in hilly zones using Surface Wetness Index (SWI) and Normalised Difference Vegetation Index (NDVI). Likewise, Lidong and Hao (2006) were used the NDVI method for water area extraction and Coa and Li (2008) used Normalized Difference Water Index (NDWI) for identification of water bodies. Fu *et al.*, (2007) developed an automatic extraction of water bodies from a Landsat TM image using DT algorithm which was based on spectral characteristics of the water body in TM images. Wang *et al.*, (2008) have developed extraction method detection of water bodies based on texture analysis. The traditional pixel based digital image classification has been and is still being used for characterization and mapping the spatial extent of water bodies (Hassan, 2014). Further, Karolina (2012) suggested that the Light Detection and Ranging (LiDAR) data is useful for measuring the water bodies at higher accuracy. The National Remote Sensing Center (NRSC, 2015) has been used the CartoDEM v3 data for preparation of vector layers of water bodies over Indian inland water bodies and sea coastline using surface flattening logic and semi-automated water bodies extraction algorithms. However, comparative detection and delineation of water bodies using CartoDEM, Shuttle Radar Topography Mission (SRTM) and Advanced Spaceborne Thermal Emission and Reflection Radiometer (ASTER) Global Digital Elevation Model (GDEM) data has been not so far attempted.

ASTER GDEM purports to be the highest resolution, 30 m (1 arc second) spacing as compare to CartoDEM and SRTM DEM (Guth, 2010). A DEM refers to a quantitative model of the earth's surface in digital form (Burrough and McDonnell, 1998) which consists of either (1) a two dimensional array of numbers that represents the spatial distribution of elevations on a regular grid; (2) a set of x, y, and z coordinates for an irregular network of points; or (3) contour strings stored in the form of x, y coordinate pairs along each contour line of specified elevation (Walker and Willgoose, 1999). Use of satellite derived DEMs have a remarkable benefits over traditional methods over large and inaccessible areas. Nowadays, it can be easily produced (near) real-time and within a relatively short time and at remarkably less costs (Jiang *et al.*, 2014). Radar Interferometric Synthetic Aperture Radar (InSAR) has recently become popular in extracting elevation data. This technique uses two or more SAR recordings to generate DEMs, using differences in the phase of the waves returning to the satellite or airborne platform (Rosen *et al.*, 2000). National Aeronautics and Space Administrations' (NASA) SRTM, which produced a near-global DEM were followed this methodology (Jiang *et al.*, 2014) for generation of DEM.

Considering the overall scenario of satellite-derived DEMs, it is hypothesized that, the satellite derived DEMs could be used for detection and delineation and monitoring the surface Water Body Area (WBA). With these views, the objective of the present attempt was to detect and delineate the WBA with its measurement based on EPF approach using available open source DEMs in GIS environment. Detection and delineation of WBA at micro level mainly in inaccessible hilly regions is difficult task possible in view of time, resources and cost issues. Therefore, the detection and delineation of water bodies were carried out using CartoDEM, SRTM and ASTER GDEM in GIS techniques. Methodology and technique formulated in this study for detection and measurement of the water bodies could be used as a rapid assessment tool for the assessment of surface water bodies especially in inaccessible areas.

2 STUDY AREA

The study area (2311km^2) encompasses of undulating topography located in the eastern hilly zone of the Western Ghats, Godavari River basin in the Maharashtra, India (Figure 1). It has complex ranges with altitude varies from 537 m to 1646 m and slope from 0° to 73° (Figure 4). There are hills linked with small scale plateau, a few of the pinnacles show greater heights; the tallest are the *Kalsubai* (1,646 m) near *Bhandardara* Dam, *Harishchandragarh* (1,422 m), *Ghanchakar Donger* (1,497m) and *Salher* (1,567m) 90 km north of Nashik. This area belongs to basaltic rocks, geological breaking and non-soils slopes. The mean rainfall is about 3000 mm receives mainly during June to October. Coarse soils are covered by dense evergreen and semi-evergreen vegetation at places with small patches of agriculture. In this area small tract of the evergreen forest mixed with deciduous forest, especially, at the western border of the region. The Godavari River is the main river receives water from different tributaries like Kadva, Darna, Pravara and Mula from both the banks. Multiple water bodies, artificial dams are located at the western side of the study area.

3 METHODOLOGY

Detection and delineation of water bodies were carried out from CartoDEM, SRTM and ASTER GDEM data with comparative analysis by following steps: (I) generation of EPF from three DEMs, (II) primary detection of water bodies, (III) preparation of contour and slope maps and its combination with EPF, (IV) conversion of detected water bodies from nearest neighbor to cubic convolution and omission of outliers EPF, (V) final detection and delineation of water bodies from three DEMs and its combination with slope and contour maps, and (VI) Comparison of detected water bodies and its validation from Landsat 8 data and topographic maps (SOI) (Figure 2).

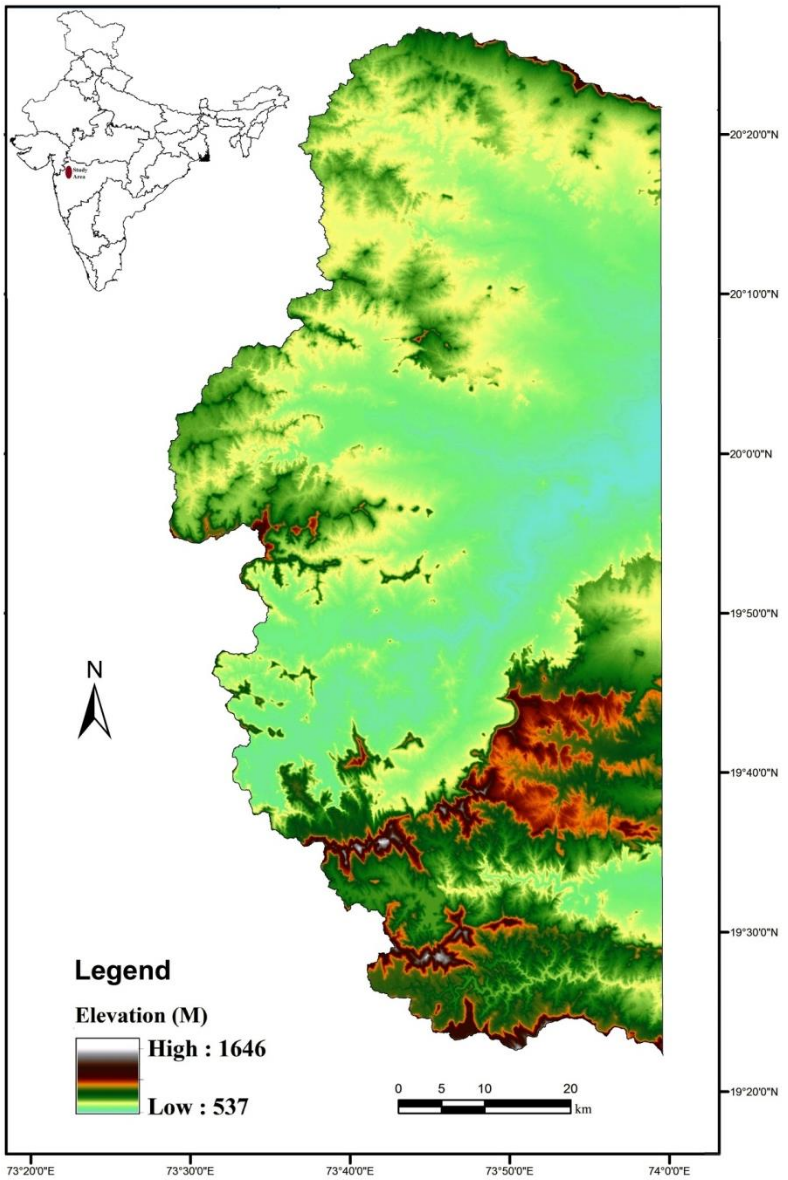

Figure 1. Location map: upper Godavari basin (ASTER image)

3.1 Database and Software used

Remotely sensed orthorectified CartoDEM, SRTM and ASTER GDEM datasets were used for detection and delineation of WBA. These DEMs could be used to monitor, detection and delineation of the surface WBA especially in inaccessible areas. For a comparative analysis of detecting and delineated water bodies, CartoDEM, SRTM and ASTER GDEM were re-projected to a common projection (UTM WGS84, Zone 43) in ArcGIS software. The 'Hydrology' toolset in ArcGIS, developed by ESRI (2004), has been used for DEM preprocessing and surface stream simulation. The precise co-registration among the DEMs is a pre-requisite because DEMs are sensitive to mis-registration for areas and relief as a shift of a fraction of a pixel may cause significant changes in the elevation difference (Ni *et al.*, 2014). Details of datasets are given in Table 1.

3.1.1 CartoDEM

The Cartosat-1 DEM (CartoDEM version 1) is an Indian DEM developed by the Indian Space Research Organization (ISRO). This DEM has been used in multiple sectors for planning and decision making. It is derived from the Cartosat-1 stereo payload launched in May 2005 by ISRO, India. The primary output is a tile of 7.5′ × 7.5′ extents with DEM spacing of 1/3 arc-sec, and co-registered ortho-image at resolution 1/12 arc-sec (NRSC, 2015). The CartoDEM is a land surface model of digital elevation and covers land and covers

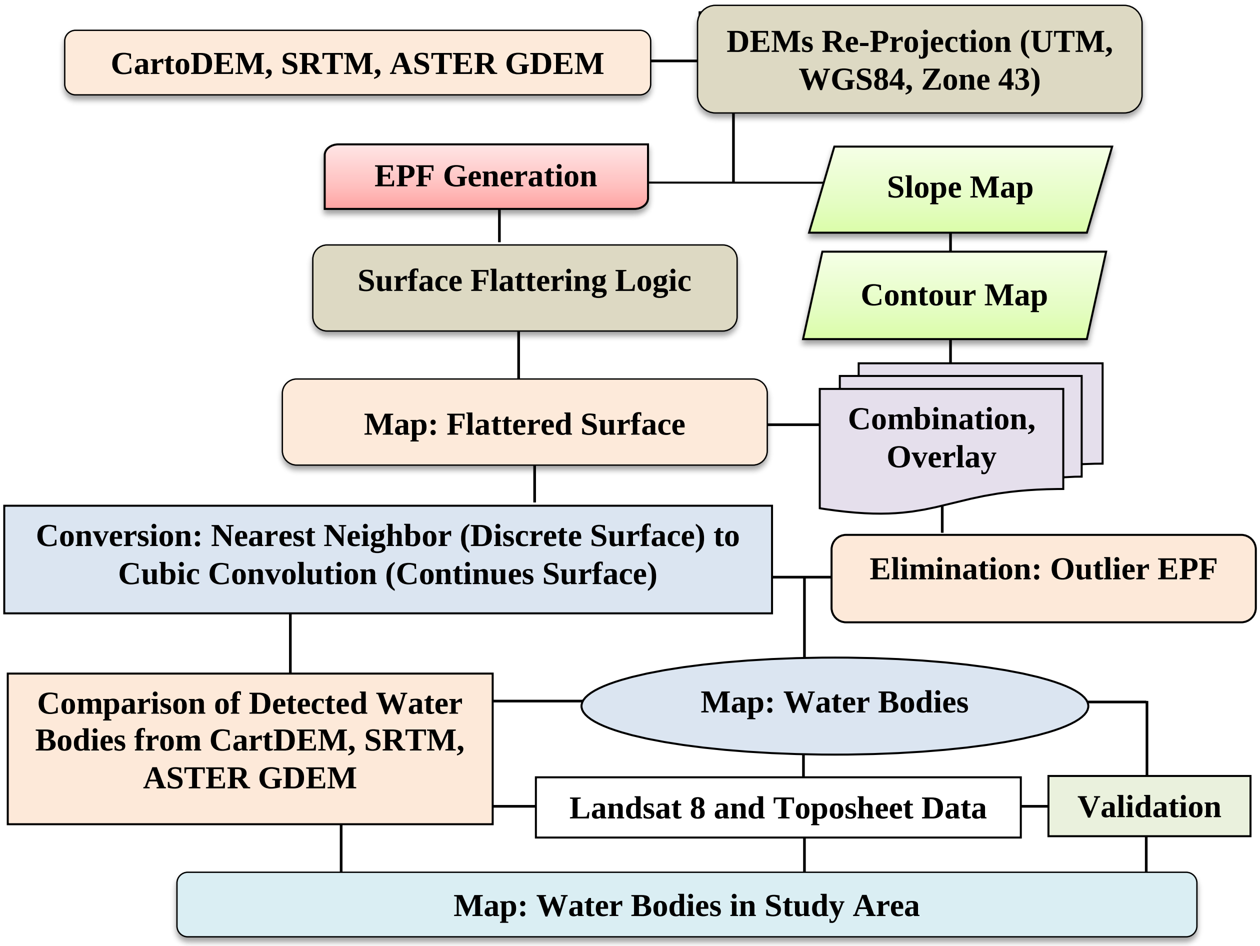

Figure 2. Schematic Preparation

Table 1. Details of used database

Database used	Spatial Resolution	Data Sources
SRTM DEM	90 meter (3-arc-second)	http://gdem.ersdac.jspacesystems.or.jp
CartoDEM V1	30 meter (1-arc-second)	http://bhuvan.nrsc.gov.in
ASTER GDEM	30 meter (1-arc-second)	http://gdem.ersdac.jspacesystems.or.jp

land surfaces within India (Das *et al.*, 2016). Freely available 1 arc second spatial resolution NRSC CartoDEM V1 and CartoDEM V1.1R1 1×1 degree tile was downloaded from the NRSC website http://bhuvan.nrsc.gov.in. The operational procedure of this DEM generation comprised of stereo strip triangulation of 500 × 27 km segment with 30-m posting (Muralikrishnan *et al.*, 2013). The vertical accuracy for CartoDEM (V1) claimed by NRSC is 8m (Muralikrishnan *et al.*, 2011). Considering the appearance of water bodies as a flatter surface over digital elevation model, this CartoDEM data was selected and used for detection of water bodies.

3.1.2 SRTM

SRTM and ASTER GDEM dataset is available at http://gdem.ersdac.jspacesystems.or.jp/ at 90m and 30m resolution. SRTM was an international project, spearheaded by the US National Geospatial-Intelligence Agency (NGA) and the National Aeronautics and Space Administration (NASA). The SRTM data provided a globally consistent digital elevation data for approximately 80% of the world's land surface area. It's produced by NASA and available at two spatial resolutions: 1-arc-second in the USA and a degraded 3-arc-second for the rest of the world. SRTM elevation data are based on the WGS84 ellipsoid as horizontal datum, while its mean sea level is defined by EGM96 geoid as vertical datum. The specified accuracy requirement for SRTM DEM products was 16m absolute vertical error (at 90% confidence level). This paper deals with the better known and widely available 3-arc-second products, which are publicly available (Jing *et al.*, 2014). Considering the smoothness in digital appearance and the visualization of WBA as a flatter surface over this DEM, this was used to achieve the objectives of the study.

3.1.3 ASTER GDEM

The ASTER GDEM purports to be the highest resolution, 30m (1 arc second) spacing as compare to CartoDEM and SRTM DEM (Guth, 2010; Arefi and Reinartz, 2011). Moreover, the ASTER sensor on board of the Terra spacecraft has an along-track stereoscopic capability due to a nadir and 27.6º backward-looking telescopes in the Near Infrared (NIR) spectral band. This instrumental setup allows for photogrammetric DEM generation with vertical accuracies of ±15-30m (Toutin, 2008). It is freely available and would make a significant contribution to understand the water bodies. ASTER GDEM is a significant for representing digital topography at 30m resolution, which was generated by stereo matching techniques, contributed by the Ministry of Economy, Trade, and Industry (METI) and NASA. Remotely sensed orthorectified ASTER GDEM (Version 1) dataset is available at free of cost from Earth Remote Sensing Data Analysis Center (ERSDAC) of Japan and NASA (ASTER GDEM, 2015). Complete GDEM covers land surfaces, which is wider than SRTM (Jing *et al.*, 2014). Topographic parameters such as elevation point, slope, aspect, cross profile can be generated using this DEM and automated procedures for detection of water bodies with cross verifications. This DEM has good spatial resolution with clear appearance of the water bodies through falter digital surface over.

Global Mapper software (v11.01) together with ArcGIS (v10.0) was used for CartoDEM, SRTM and ASTER GDEM data processing, i.e. generation of EPFs (7194906), slope and contour map preparation. The obtained results from the EPFs, slope map and contour map were cross-validated from Landsat 8 satellite imagery (Dec 2013) and topographical maps (No. 47/E/5 and 47/E/9) obtained from Survey of India (SOI). Moreover, these water bodies were also verified from high-resolution Google Earth images. It is a complementary reference to help distinguish confusing water bodies from background noise like mountain shadows (Jiang *et al.*, 2014).

3.2 Approaches

3.2.1 EPF Approach

The smooth water bodies act as specular reflector and thus reflect most of the transmitted energy from the sensor that results the low backscatter values from water bodies (Hahmann *et. al.*, 2008). Such water bodies are digitally appearing as flattening surface over inland water bodies on CartoDEM, SRTM and ASTER GDEM. In some cases, the water bodies may be normalized to have a slope value around zero degree. Therefore, the flattening surface over these DEMs is considered as water bodies that may be reservoir, lake, dam, etc. over inland surface. Scientifically, each and every water bodies are smooth and plain because of its liquid nature. Thus, water bodies are absolutely smooth and flat (Slope: 0°-0.5°) appeared on these DEMs images as compare to other region were considered as water bodies. Flat digital pixels over CartoDEM, SRTM and ASTER GDEM are seemed, as a water body (Frey and Paul, 2011) which can be used to detect the surface water body area (WBA) using slope and contour maps using combination logic.

EPF is the grid points which are generated in unique array and consisted with specific height on the DEMs. It is the grid point which has the unique elevation value at specific intervals. In this study, CartoDEM, SRTM and ASTER GDEM data were processed for generation of EPFs (Figure 3). Conceptually, the unique DEM values (EPF) are picked up along the boundaries of water body as an input for determining the elevation of each water body. The logic behind unique EPFs is the flattening surface. Each of the water body has assigned flat elevation value in the DEMs. The EPF (7194906) was created at Elevation Grid Cell Centers (EGCC) by automated procedures (Figure 3). Spatial query was run in the query builder over the selected DEMs sample EPF for detection of the WBA in the selected study area. Generated EPFs were exported into point vector data shape file and put up in the software for further processing as quarry analysis. In the entire EPFs few outlier (non-water body) points are occurred due to unique elevation with the existed WBA. These identical spatial heights were an error with relevant water bodies in the surrounding area. Thus, the data combination approach was used to remove the non-water bodies' points.

3.2.2 Combination Approach

Generated EPFs are integrated with prepared contour and slope map using query analysis task by combining the generated 7194906 EPFs. The contour and slope maps were used to detect the WBA (Figure 4). Example: the contour line (576m) detection at the edge of water bodies of Darna reservoir (Figure 5) was performed for cross verification of obtaining results from advance query and combination of slope map. The slope map with 0° to 0.5° was used to compare the WBA in the existed EPFs cluster. This detected EPFs (590m and 576m) area was cross-validated from Landsat 8 satellite imagery and topographical maps of the same region. The omission of unnecessary EPF (non-water bodies) is essential to measure the WBA, precisely. The delineation of contour at the edges of water bodies and its incorporation with slope map was therefore attempted (Figure 5). These were the non-clustered points (non-water bodies) and located in the outlier part of the existed water bodies. For the purpose of clear identification of boundaries of water bodies, nearest neighbor (for discrete surface) to cubic convolution (for continues surface) conversion of DEMs were carried out (Figure 6). Finally, the combination of EPFs, slope map, recognition of contour line at the edge of water bodies and nearest neighbor to cubic convolution of processed DEMs were attempted for final detection of the water bodies in the study area (Figure 7).

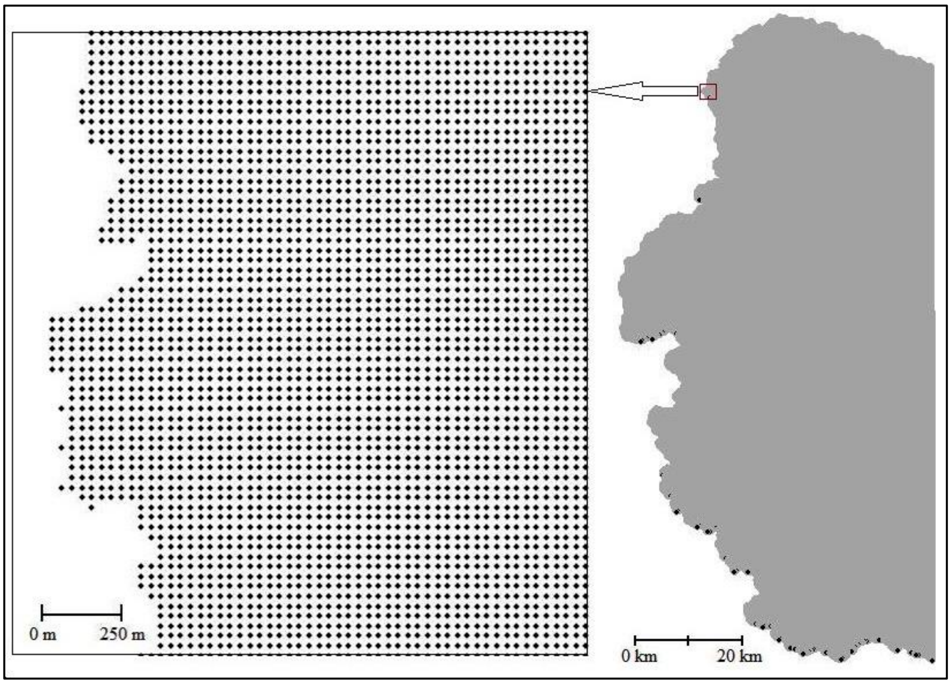

Figure 3. Elevation Points Feature (EPF) from ASTER GDEM

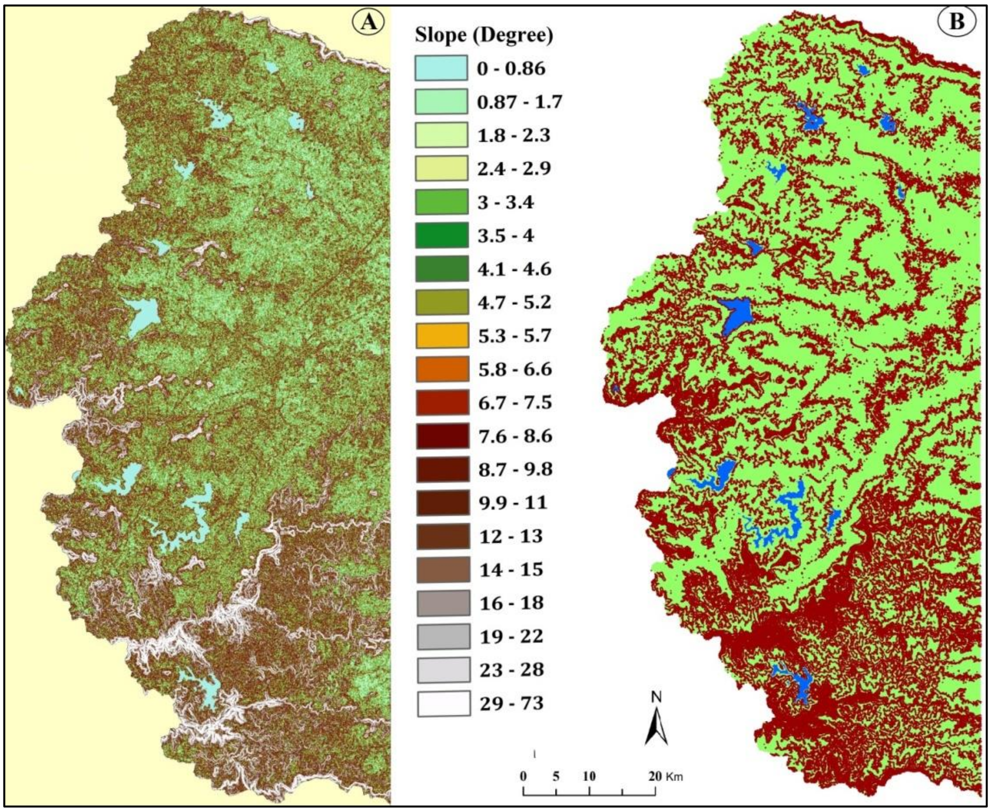

Figure 4. (A) Slope map; (B) Superimposing of contour line (Interval: 100 m) over the water bodies

4 RESULT AND DISCUSSION

4.1 EPF Result

The water bodies are digitally appearing over the 3 DEMs as a flattening surface. The digital topography seemed with flattering digital pixels (Frey and Paul, 2011) on the selected DEMs can be consider as WBA. The selected DEMs were processed for EPFs generations (7194906). The generated EPFs are unique height vector points, distributed with same interval over these DEMs. The heights of all EPFs were found same, which was considered as the WBA. Derived slope and contour from DEMs are probably useful for the visual appearance of WBA. Available ASTER GDEM and CartoDEM purports to be the highest resolution, with 30 m (1 arc second) spacing (Guth, 2010) as compare to SRTM data, thus, the smooth water bodies act as precise specular reflectors over these DEMs. Hence, the outcome of the precise resolution from ASTER GDEM and CartoDEM were better for detection and delineation of water bodies in the area. SRTM data overestimate the elevations. For SRTM, overestimation of elevation is predictable since radar signal returns are affected by vegetation cover (Guth, 2006; Shortridge 2006). It might be because of the spatial resolution of the same data. Therefore, large error was noticed in the water body detection from the SRTM data (Figure 7). These errors mean, highlighting the non-water body area over the SRTM DEM. Probably, the EPFs are without the clustering precincts over SRTM data as compare to ASTER and CartoDEM data.

4.2 Data Combination

Identical height of water bodies EPFs are seen in the surrounded non-water body area which could be an error in the present assessment. In view of this, in the current task, from the spatial quires results the shape of EPF was found irregular due to the location of water bodies is consisted with undulating hilly topography in the study area. The result reveled from spatial query on EPFs for Dam 1 and Dam 2 sites were shown the water body area with unnecessary EPFs as an error points (Figure 5). Thus, for appropriate detection of water bodies with the slope and contour map combination increased the preciseness in the WBA. The slope maps generated from CartoDEM, SRTM and ASTER GDEM were also supported for water body detection. In this sense, the slope is absolutely plain between 0° to 0.5°; flattening the surface of DEMs, absence of contours in the WBA and clustering of EPFs in the area logic helped to detect the precise water bodies in the area. The data combination approach improves the result of WBAs appearance. At the same time, the

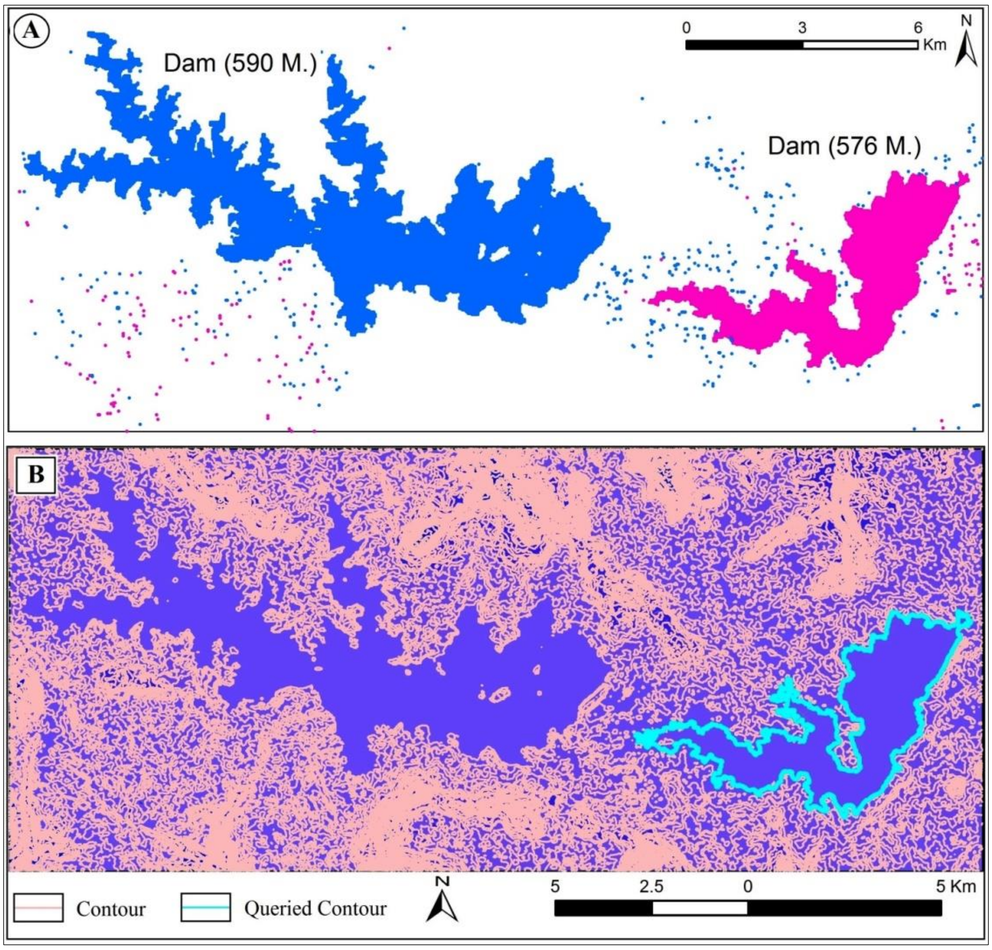

Figure 5. (A) Primarily detected water bodies by query analysis with outlier EPF; (B) Detected water bodies by combining contour and advance spatial query

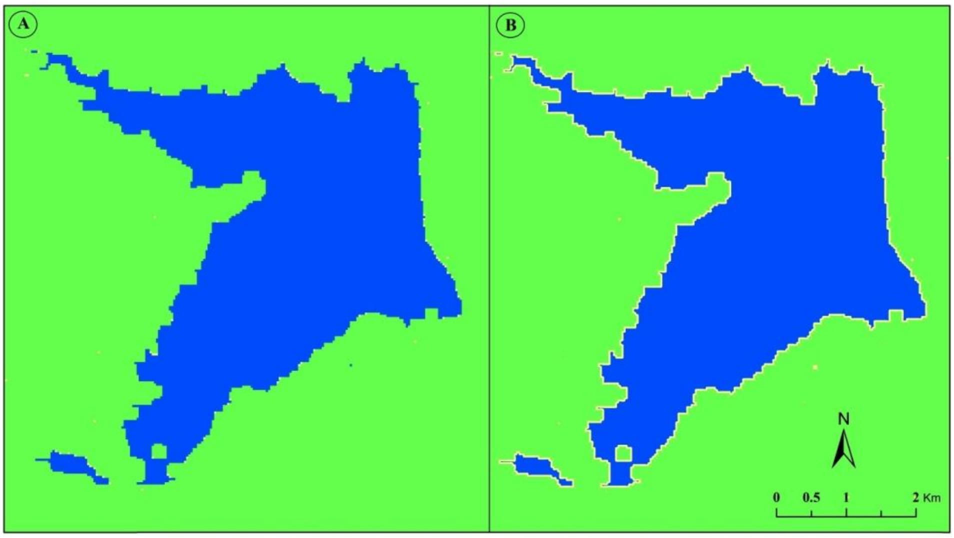

Figure 6. Nearest neighbor to cubic convolution conversion for detecting the edges of water bodies: (A) water bodies with nearest neighbor; (B) water bodies with cubic convolution

conversions of detecting WBA from the nearest neighbor to cubic convolution were also helped to enhance the detected water bodies after the appearance of proper boundary of water bodies (Figure 6). To avoid the bias delineation the incorporated approach of slope, contour and its cross validation from high resolution satellite imagery, etc. are more supportive to enhanced detection and delineation of the WBA in the present hilly region.

4.3 Detection and Delineation of Water Bodies

Results obtained for the selected water bodies indicating that, both CartoDEM and ASTER GDEM data meet their predefined vertical accuracy specifications as compare to SRTM data. It was realized that ASTER GDEM data and CartoDEM have a higher horizontal accuracy than SRTM for the study area. In this study, these spatial and vertical resolutions of both the dataset are influencing the preciseness of detected WBA. The underestimation of ASTER and CartoDEM is more pronounced on flat and less complex terrain and of a greater magnitude than the overestimation of SRTM (Gerald and Ben, 2012). Water bodies are appeared similar over all DEMs: SRTM 90m, ASTER 30m and CartoDEM 30m. This comparison shows that DEMs data can be used to detect the water bodies precisely. However, WBA could be detected from CartoDEM and ASTER GDEM with precision. The distribution analysis shows bias estimation using DEM using SRTM data with less precision. Assimilation of query analysis, contour line delineation at the edge of water bodies, clustering of EPF, non-contour area and flattening water bodies over ASTER GDEM and CartoDEM with 0° to 0.5° slope area were finally considered as WBA in the present study area (Figure 7). Water bodies in the study area were estimated as: 3.09% of reviewed area from CartoDEM, 2.22% from ASTER GDEM and 4.38% from SRTM DEM (Table 2). CartoDEM and ASTER GDEM show potentials of precise estimation of surface water bodies especially in inaccessible hilly region as it has higher resolution and good digital flattering surface texture. However, smaller water bodies have been detected and delineated more precisely from CartoDEM (v1) than ASTER GDEM.

Table 2. Detected WBA (%) from DEMs

DEM	WBA (%)
SRTM DEM	4.38
ASTER GDEM	2.22
CartoDEM (v1)	3.09

5 CONCLUSION

The detection and delineation of water bodies provide the information base for planning of water resource issues. CartoDEM, SRTM and ASTER GDEM were used for detection and delineation of WBA after the estimation of EPFs, slope values, contours and its assimilation with spatial and advance query approach. The detection of precise water bodies in the hilly area might be a massive task due to hilly nature, slope and dense vegetation cover. The CartoDEM and ASTER GDEM data were useful for the detection and delineation of water bodies with due care (elimination of neighboring unnecessary EPF), especially at inaccessible area. The detection of faltering surface by similar elevation points (water bodies) and elimination of neighboring unnecessary (non-water bodies) EPF is

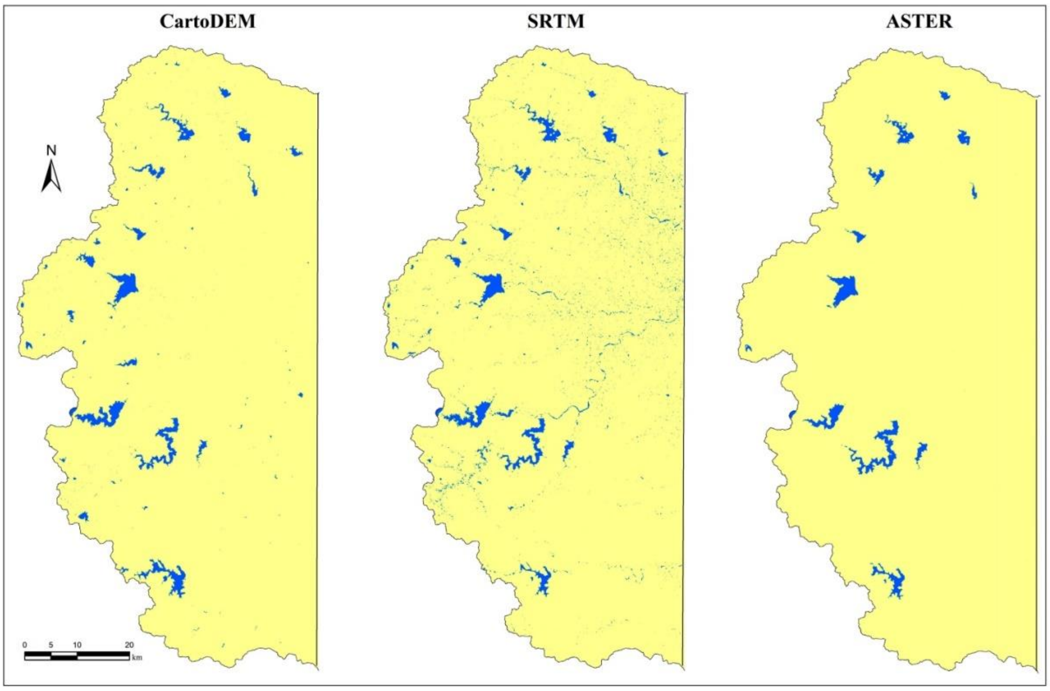

Figure 7. Detected Water Bodies from CartoDEM, SRTM and ASTER GDEM data

considered as one of the first steps towards obtaining an accurate water bodies from DEMs data. The area is absolutely smooth and flattening (Slope: 0°-0.5°), which could be a non-contour area over the selected DEMs as compared to other digital topography is considered as WBA. About 3.09 % of the reviewed area has been estimated as water bodies from CartoDEM. Further, CartoDEM was the best alternative for detection of small water bodies (Figure 7) as compare to ASTER GDEM and SRTM. Therefore, CartoDEM were stood more appropriate as compared to ASTER GDEM and SRTM DEM for precise detection of WBA in hilly areas. The methodology used in this study could become an effective and rapid assessment tool prior to water resource management using remote sensing data.

CONFLICT OF INTEREST

The authors declare no conflict of interest.

ACKNOWLEDGEMENTS

Authors are thankful to Department of Geography, S.N. Arts, D.J.M. Commerce and B.N.S. Science College, Sangamner, Maritime, Technology and Environment Hub, Research and Innovation, Southampton Solent University, and Department of Geography, H.P.T. Arts and R.Y.K. Science College, Nashik, for support and providing necessary research facilities. Author gratefully acknowledge the anonymous reviewers for constructive comments and suggestions for improvement in the draft.

ABBREVIATIONS

ASTER: Advanced Spaceborne Thermal Emission and Reflection; **DEM**: Digital Elevation Model; **EGCC**: Elevation Grid Cell Centers; **EPF**: Elevation Point Feature; **GDEM:** Global Digital Elevation Model; **GIS:** Geographical Information System; **InSAR:** Interferometric Synthetic Aperture Radar; **ISRO**: Indian Space Research Organisation; **NASA**: National Aeronautics and Space Administration; **NDVI**: Normalized Difference Vegetation Index; **NDWI**: Normalized Difference Water Index; **NRSC**: National Remote Sensing Centre; **SRTM**: Shuttle Radar Topography Mission; Water Body Area; **WGS**: World Geodetic System.

REFERENCES

Aher, S. P., Shinde, S. D., Guha, S. and Majumder, M., 2017 Identification of Drought in Dhalai River Watershed using MCDM and ANN Models. *Journal of Earth System Science*, 126, 1-14.

Aher, S. P., Bairagi, S. I., Deshmukh, P. P. and Gaikwad, R. D., 2012. River change detection and bank erosion identification using topographical and remote sensing data. *International Journal of Applied Information System* 2, 1-7.

Akhtar, A. M., Sher, M., Said, R. and Mateeul, H., 2015. Flood monitoring and damage assessment using water indices: A case study of Pakistan flood-2012. *The Egyptian Journal of Remote Sensing and Space Science*, 18(1), 99-106.

Arefi, H. and Reinartz, P., 2011. Accuracy Enhancement of ASTER Global Digital Elevation Models Using ICESat Data. *Remote Sensing*, 3, 1323-1343.

ASTER GDEM-1999. ASTER GDEM Readme File – ASTER GDEM Version 1. (accessed in April 2015).

Barbara, T.-W., Aher, S.P., Gawali, P.B. and Laxmi, B.V., 2016. Seismic Hazard Analysis along Koyna Dam Area, Western Maharashtra, India: A Contribution of Remote Sensing and GIS. *Geosciences*, 6, 1-20.

Bhagat, V. S. and Sonawane, K. R., 2011. Use of Landsat ETM+ data for delineation of water bodies in hilly zones. *Journal of Hydroinformatics*, 13, 661-671.

Bhagat, V. S., 2009. Use of Landsat ETM+ data for detection of potential areas for afforestation. *International Journal of Remote Sensing*, 30, 2607-2617.

Brisco, B., Schmitt, A., Murnaghan, K., Kaya, S. and Roth, A., 2013. SAR polarimetric change detection for flooded vegetation. *International Journal of Digital Earth*, 6, 103-114.

Burrough, P. A. and McDonnell, R. A., 1998. Principles of Geographic Information Systems, 333, New York: Oxford University Press.

Cao, R., Li, C., Liu, L. Wang J. and Yan, G., 2008. Extracting Miyun reservoir's water area and monitoring its change based on a revised normalized different water index. *Science of Surveying and Mapping*, 33, 158-160.

Carroll, M. L., Townshend, J. R. G., DiMiceli, C. M., Loboda, T. and Sohlberg, R. A., 2011. Shrinking Lakes of the Arctic: Spatial Relationships and Trajectory of Change. *Geophysical Research Letters*, 38 (L20406), 1-5.

Cole, J. J., Prairie, Y. T., Caraco, N. F., McDowell, W. H., Tranvik, L. J., Striegl, R. G., Duarte, C. M., Kortelainen, P., Downing, J. A., Middelburg, J. J. and Melack, J., 2007. Plumbing the Global Carbon Cycle: Integrating Inland Waters into the Terrestrial Carbon Budget. *Ecosystems*, 10,172-185.

Das, S., Patel, P.P. and Sengupta, S., 2016. Evaluation of different digital elevation models for analyzing drainage morphometric parameters in a mountainous terrain: a case study of the Supin–Upper Tons Basin, Indian Himalayas. *Springer Plus*, 5 (1544), 1-38.

Demir, B., Bovolo, F. and Bruzzone, L., 2013. Updating land-cover maps by classification of image time series: A novel change-detection-driven transfer learning approach. *IEEE Transactions, Geoscience and Remote Sensing*, 51, 300-312.

Deshmukh, K. K. and Aher S. P, 2016. Assessment of the Impact of Municipal Solid Waste on Groundwater Quality near the Sangamner City using GIS Approach. *Water Resource Management*, 30 (7), 2425-2443.

Deshmukh, K., Aher, S., Gawali, P. and Deshmukh, P., 2017. Groundwater quality in Deccan upland region along the Mulmala Stream, Chandanapuri Valley, Sangamner, Maharashtra, India. *Sustainable Water Resources Management*, 1-11.

Dronova, I., Gong, P. and Wang, L., 2011. Object-based analysis and change detection of major wetland cover types and their classification uncertainty during the low water period at Poyang Lake, China. *Remote Sensing Environment*, 115, 3220-3236.

Du, Z., Linghu, B., Ling, F., Li, W., Tian, W., Wang, H., Gui, Y., Sun, B. and Zhang, X., 2012. Estimating surface water area changes using time-series Landsat data in the Qingjiang river basin, China. *Journal of Applied Remote Sensing*, 6, 1-16.

ESRI, 2004. Environmental Systems Research Institute, Arc hydro tools overview. ESRI, United States of America.

Famiglietti, J. S. and Rodell, M., 2013. Water in the Balance. *Science,* 340, 1300-1301.

Feng, M., Sexton, J. O., Channan, S. and Townshend, J. R., 2015. A global, high-resolution (30-m) inland water body dataset for 2000: first results of a topographic–spectral classification algorithm. *International Journal of Digital Earth*, 113-133.

Frey, H. and Paul, F., 2011. On the suitability of the SRTM DEM and ASTER GDEM for the compilation of topographic parameters in glacier inventories. *International Journal of Applied Earth Observation and Geoinformation*, 18, 480-490.

Fu, J., Wang, J. and Li, J., 2007. Study on the Automatic Extraction of Water Body from TM Image Using Decision Tree Algorithm. *Proceedings of the International Symposium on Photoelectronic Detection and Imaging: Technology and Applications 2007: Related Technologies and Applications*, *Beijing*, 9-12.

Gawali, P. B., Aher, S. P., Lakshmi, B. V., Gaikwad, R. D., Deendayalan, K., Hanamgond, P. T., Mahesh Babu, J. L. V., Arote, S. A. and Bairage, S. I., 2017. Identification of Landslide Susceptible Villages around Kalsubai Region, Western Ghats of Maharashtra using Geospatial Techniques. *Journal of the Geological Society of India*, 90, 259-384.

Gerald, F. and Ben, M., 2012. Comparison of SRTM and ASTER Derived Digital Elevation Models over Two Regions in Ghana. *Implications for Hydrological and Environmental Modeling, Studies on Environmental and Applied Geomorphology (Edited by Dr. Tommaso Piacentini), InTech*, 220-240.

Guth, P. L., 2006. Geomorphometry from SRTM: Comparison to NED. *Photogrammetric Engineering and Remote sensing* 72 (3), 269-277.

Guth, P. L., 2010. Geomorphometric Comparison of ASTER GDEM and SRTM. *A special joint symposium of ISPRS Technical Commission IV and AutoCarto in conjunction with ASPRS/CaGIS, Orlando, Florida*.

Hahmann, T., Martinis, S., Twele, A., Roth, A. and Buchroithner, M., 2008. Extraction of water and flood areas from SAR data. *Proceedings of 7th European Conference on Synthetic Aperture Radar (EUSAR),* Friedrichshafen, Germany, 1, 177-180.

Hassan, N., Hamid, J. R. A., Adnan, N. A. and Jaafar, M., 2014. Delineation of Wetland Areas from High Resolution World View-2 Data by Object-Based Method. *Proceedings of the IOP Conference Series: Earth and Environmental Science*, 18, Article ID: 012017.

Ho, L. T. K., Umitsu, M. and Yamaguchi, Y., 2010. Flood Hazard Mapping by Satellite Images and SRTM DEM in the VU GIA Thu Bon Alluvial Plain, Central Vietnam. *International Archives of the Photogrammetry, Remote Sensing and Spatial Information Science*, 38, 275-280.

ISRO [Indian Space Research Organisation] and NRSC [National Remote Sensing Center], 2011. *Evaluation of Indian National DEM from Cartosat-1 Data, Summary Report Version 1*, Hyderabad.

Jawak, S.D. and Luis, A. J., 2013. Improved land cover mapping using high resolution multiangle 8-band WorldView-2 satellite remote sensing data. *Journal of Applied Remote Sensing*, 7, 073573, DOI: 10.1117/1.JRS.7.073573.

Jiang, H., Feng, M., Zhu, Y., Lu., N., Huang, J. and Xiao, T., 2014. An Automated Method for Extracting Rivers and Lakes from Landsat Imagery. *Remote Sensing*, 6, 5067-5089.

Jing, C., Shortridge, A., Lin, S. and Wu, J., 2014. Comparison and validation of SRTM and ASTER GDEM for a subtropical landscape in Southeastern China. *International Journal of Digital Earth*, 7 (12), 969-992.

Kaliraj, S., Muthu, M. S. and Malar, V. K., 2012. Application of remote sensing in detection of forest cover changes using geo-statistical change detection matrices-A case study of Devanampatti reserve forest, Tamilnadu, India. *National Environment Pollution Technology* 11, 261-269.

Karolina, K., 2012. Modelling of water surface topography on the DEMs, Multidisciplinary Research on Geographical Information in Europe and beyond. *Proceedings of the AGILE' 2012 International Congress of Geographic Information Science*, Avignon, 24-27.

Lidong, D. and Hao, W., 2006. Study of the water body extracting from MODIS images based on spectrumphotometric method. *Geomatics and Spatial Information Technology*, 29, 25-27.

Markogianni, V., Dimitriou, E. and Kalivas, D. P., 2013. Land-use and vegetation change detection in Plastira artificial lake catchment (Greece) by using remote-sensing and GIS techniques. *International Journal of Remote Sensing*, 34, 1265-1281.

Meijerink, A. M. J., 1996. Remote sensing applications to hydrology: groundwater. *Hydrological Sciences Journal,* 41, 549-561.

Min, L., Xu, L. and Min, T., 2011. An Extraction method for Water Body of Remote Sensing Image Based on Oscillatory Network. *Journal of Multimedia,* 6, 252-260.

Muralikrishnan, S,, Narender, B, Reddy, S and Pillai, A., 2011. Evaluation of Indian National DEM from Cartosat-1 data. *National Remote Sensing Center. Hyderabad: Indian Space Research Organisation.*

Muralikrishnan, S, Pillai, A, Narender, B, Reddy, S, Venkataraman, V. R. and Dadhwal, V. K., 2013. Validation of Indian National DEM from Cartosat-1 data. *Journal of Indian Society Remote Sensing,* 41, 1-13.

Ni, W., Sun, G., Zhang, Z., Guo, Z. and He, Y., 2014. Co-registration of two DEMs: impacts on forest height estimation from SRTM and NED at mountainous areas. *IEEE Geosciences Remote Sensing Lett.*, 11:273-277.

NRSC [National Remote Sensing Centre, ISRO], 2015. Water bodies flattening, Technical report. *National remote sensing center, Hyderabad*, India.

Ridda, M. K. and Liu, J., 1998. A comparison of four algorithms for change detection in an urban environment. *Remote Sensing Environment,* 63, 95-100.

Rokni, K., Ahmad, A., Selamat, A. and Hazini, S., 2014. Water Feature Extraction and Change Detection Using Multitemporal Landsat Imagery. *Remote Sensing,* 6, 4173-4189.

Rosen, P. A., Hensley, S., Joughin, I. R., Li, F. K., Madsen, S. N., Rodriquez, E. and Goldstein, R. M., 2000.

Synthetic aperture radar interferometry. *Proceedings of the IEEE*, 88, 333-382.

Salmon, B. P., Kleynhans, W., Van Den Bergh, F., Olivier, J. C., Grobler, T. L. and Wessels, K. J., 2013. Land cover change detection using the internal covariance matrix of the extended Kalman filter over multiple spectral bands. *IEEE Journal Sel. Topics Application Earth Observations Remote Sensing*, 6, 1079-1085.

Shortridge, A., 2006. Shuttle Radar Topography Mission Elevation Data Error and Its Relationship to Land Cover. *Cartography and Geographic Information Science* 33 (1), 65-75.

Sun, F., Sun, W., Chen, J. and Gong, P., 2012. Comparison and improvement of methods for identifying waterbodies in remotely sensed imagery. *International Journal of Remote Sensing*, 33, 6854-6875.

Tang, Z., Ou, W., Dai, Y. and Xin, Y., 2013. Extraction of water body based on Landsat TM5 imagery-A case study in the Yangtze River. *Advance Information Communication Technology*, 393, 416-420.

Toutin, T., 2008. ASTER DEMs for geomatic and geoscientific applications: a review. *International Journal of Remote Sensing* 29 (7), 1855-1875.

Volpi, M., Petropoulos, G. P. and Kanevski, M., 2013. Flooding extent cartography with Landsat TM imagery and regularized Kernel Fisher's discriminant analysis. *Computer Geoscience*, 57, 24-31.

Walker, J. P. and Willgoose, G. R., 1999. On the effect of digital elevation model accuracy on hydrology and geomorphology. *Water Resources Research*, 35, 2259-2268.

Wang, H., Pan, L. and Zheng, H., 2008. Multi-Texture-Model for Water Extraction Based on Remote Sensing Image. *Proceedings of the Congress on Image and Signal Processing, Sanya*, 710-714.

Xu, H., 2006. Modification of normalised difference water index to enhance open water features in remotely sensed imagery. *International Journal of Remote Sensing*, 27, 3025-3033.

Zhu, X., Cao, J. and Dai, Y. A., 2011. Decision Tree Model for Meteorological Disasters Grade Evaluation of Flood. *Proceedings of 4th International Joint Conference on Computational Sciences and Optimization*, New York, USA, 916-919.

******